SUPPLEMENTARY INFORMATION

Materials and Methods

Fibres and particles

The panel of particles investigated consisted of 4 different samples of multi-walled carbon nanotubes (herein simply referred to as NT) and 3 control particles, which consisted of mixed length amosite asbestos enriched for long fibres (50.36% fibres >15 µm, 35.25% fibres >20 µm), hereafter referred to as long fibre asbestos (LFA), shortened amosite asbestos (SFA; 4.46% fibres >15 µm, 0.99% fibres >20 µm), and nano-carbon black (NPCB). Both LFA and SFA were created from the same batch of South African amosite[1] obtained from the Manville Corporation (USA). SFA was prepared by grinding long fibres in a ceramic ball mill, and the resulting fibre preparation sedimented in water. The process of ball milling, used to shorten the LFA to make the SFA was associated with changes in the iron chemistry[2].

The NT utilised were chosen for different physical characteristics that allowed us to address the hypothesis in hand. The samples consisted of a commercially produced long fibre NT sample ($NT_{long1;}$ Mitsui & Co. Ltd., Japan) produced by catalytic chemical vapour synthesis using the floating reaction method. A NT sample of predominantly long fibres (NT_{long2}) was used, produced in an academic research laboratory (University of Cambridge) using catalytic vapour discharge (CVD) method using a ferrocene-toluene feedstock to grow nanotubes from iron catalysts held on a silica plate[3]. These nanotubes grew aligned as mats, meaning they were straight and un-entangled. The nanotubes were harvested from the mats using a razor blade, with some residual iron remaining within the nanotubes. We also included two

commercially available curled and tangled nanotubes of different lengths (NT_{tang1} which was cut to form predominantly short NT fibres and the original length NT sample (NT_{tang2}); NanoLab, Inc., MA, USA). These were produced by CVD with an iron and ceramic oxide (alumino-silicate) catalyst support which was removed using HCl and Hydrofluoric acid treatment.

The levels and types of contaminating metals contained within the samples were established using inductively coupled plasma mass spectrometry (ICP-MS) analysis using a iCAP 6500 (Thermo Scientific, MA, USA). To evaluate the total metal contaminants (data shown in supplementary Fig. 1), the samples were acid digested in 5 ml of HNO_3, boiled down to a volume of 1 ml and 4 ml of HCL then added. This gave a final concentration on 4% HNO_3 : 16% HCL. To establish the degree of soluble metal contamination, a soluble fraction was prepared by suspending the samples in distilled H_2O prior to mixing and filtration to remove particulates and the supernatant analysed. The presence of bacterial contamination of the particle panel was established by measuring endotoxin levels. Briefly a 1 mg/ml solution of each particle was mixed on a rotating mixer at room temperature for 24-hrs prior to ultra centrifugation of the sample (13,800g). The endotoxin level of the supernatant was established using a chromogenic limulus ameobocyte lysate (LAL) assay (Cambrex Bio Science Walkersville, Inc, MD) with a limit of detection of 10 pg/ml.

To establish the physico-chemical characteristics of the particles and to identify which samples contained considerable numbers of long fibres, we utilised scanning electron microscopy (SEM), transmission electron microscopy (TEM) and light microscopy (only TEM images are shown for

reasons of brevity) where appropriate to fully describe each sample (Table 1). Using measurement software (Image-Pro Plus; Media Cybernetics Inc., MD, USA), we were able to measure diameter of both individual fibres and, in the case of NT_{tang1} and NT_{tang2}, agglomerate size as well as a length size distribution analysis of the fibres and particles used. In keeping with World Health Organization (WHO) guidelines[4] we counted only those particles with a length to width ratio greater than 3:1 and a length more than 5 µm as a fibre.

Necessarily different suspension media were required for suspending particles for injection *in vivo* (dispersion in a protein solution) and for electron microscopy (dispersion in a solvent). In preparation for electron microscopy, particles were suspended in propan-2-ol (Fisher Chemicals) and the aggregates gently exfoliated using an ultra-sonicating water bath. The sample suspensions were then diluted into 1.25 % propan-2-ol/ de-ionised H_2O (Milli-Q Academic, Millipore, MA, USA) solution. The suspension was then placed onto 1x2 mm copper slot grids pre-coated with a Formvar/ carbon film (Agar Scientific, Essex, UK), allowed to dry and analysed using a Philips CM120 transmission electron microscope.

Dispersal of NTs for in vivo experiments

There have been several published methodologies for the dispersion of NT using organic solvents or polymers[5,6]. The nature of these dispersants means that, whilst they are in some cases very effective at creating stable NT dispersions, they are often unsuitable for use in a biological system due to inherent toxicity. An alternative was sought and suspension of the particles in 0.5 % bovine serum albumin (BSA; Sigma-Aldrich, Poole, UK)/ saline solution with 2-hrs in an ultra-sonicating water bath proved to be an effective method

of dispersal. Comparison of the 0.5 % BSA/ Saline vehicle with saline alone by intraperitoneal injection into female C57Bl/6 mice (0.5 ml) produced no increase in inflammatory cells or total protein (data not shown). As such, it was deemed a suitable non-pathogenic vehicle for particle instillation

Experimental Animals

Female C57BL/6 mice aged 8 weeks were intraperitoneally injected with 0.5 ml of 100 µg/ml NPCB, SFA, LFA, NT_{tang1}, NT_{tang2}, NT_{long1} or NT_{long2} for either 24-hrs or 7-days. The particles were suspended in a sterile 0.5 % BSA/ saline solution (included as a vehicle control; 0.5 ml), allowing for an overall exposure of 50 µg per mouse. In order to ascertain if a soluble component could be responsible for the inflammogenicity seen in samples $NT_{long}1$ and $NT_{long}2$, soluble fractions of $NT_{long}1$ and $NT_{long}2$ samples were made. A 100 µg/ml suspension of each sample was made using a 0.5 % BSA/ Saline vehicle and placed in an ultra-sonicating water bath (230V, 50/60 Cycles; Kontes BP-1, NJ, USA) for 2-hours to disperse the nanotubes. This was followed by continuous mixing of each nanotube sample at 37°C over night prior to centrifugation of the sample at 16,200g for 5 minutes to remove the nanotubes leaving the extract supernatant. A single dose of 0.5 ml of either nanotube extract or vehicle control was administered intraperintoneally to female C57Bl/6 mice and the inflammatory response evaluated after 24-hrs (supplementary Fig. 2).

Cells

At each time point the mice were sacrificed by cervical dislocation and the peritoneum lavaged three times using 2 ml washes of sterile ice-cold saline. The lavages were pooled together and placed on ice for the entire duration of

the processing. The lavage fluid was then centrifuged at 123g for 5 minutes at 4°C in a Mistral 3000i centrifuge (Thermo Fisher Scientific, Inc., MA, USA) and an aliquot of the supernatant was retained for total protein measurement. The remaining supernatant was discarded and the cell pellet re-suspended in 0.5 ml of 0.1 % BSA/ sterile saline solution. A total cell count was then performed using a NucleoCounter (ChemoMetec, A/S, Allerød, Denmark). Differential cell counts were performed on cyto-centrifugation preparations, stained with Diff Quik. Images of cells (fig. 2 a-f) were taken using QCapture Pro (Media Cyberbernetics Inc., MD, USA).

Total protein concentration of the peritoneal lavage fluid was measured using the bicinchoninic acid (BCA) protein assay (Sigma-Aldrich, Poole, UK). Sample protein concentrations were established by comparison to a BSA standard curve (0 – 1000 µg/ml). The samples were then incubated at 37ºC for 30 minutes after the addition of the test reagent (1 part Copper (II) Sulphate solution (4 % w/v) to 50 parts bicinchoninic acid). The absorbance was then read at 570 nm using a Synergy HT microplate reader (BioTek Instruments, Inc. VT, USA) and the sample protein concentration established via extrapolation from the BSA standard curve.

Dissection and fixation of diaphragm

Following sacrifice and peritoneal lavage at 7-day time point, the abdominal wall was dissected free, exposing the peritoneal cavity via a midventral incision with lateral incisions extending to the veterebral column, which was then severed below the diaphragm. The diaphragm was then carefully removed by cutting through the ribs and chest wall with care taken not to puncture the diaphragm. The diaphragm was gently rinsed three times by

emersion in ice-cold sterile saline and placed overnight into methacarn fixative (60 % methanol, 30 % chloroform and 10 % glacial acetic acid) for histological staining or 3 % glutaraldehyde/ 0.1 M sodium cacodylate (pH 7.2) buffer for SEM. After overnight incubation in fixative, the diaphragm was carefully excised from the surrounding ribs prior to further processing for either histological or SEM analysis.

Methodology for quantifying granulomas

After removal from the ribs, the same full width section of the upper quadrant of the diaphragm was removed from each animal sampled so as to encompass both muscular and central tendinous regions of the diaphragm. This excised tissue was dehydrated through graded alcohol (ethanol) and imbedded on-edge in paraffin. Four µm sections of the diaphragm were stained with hematoxylin and eosin stain and serial images taken at x100 magnification using QCapture Pro software (Media Cyberbernetics Inc., MD, USA). The images were seamlessly re-aligned using Photoshop Elements 4 (Adobe systems Inc.) to give a high resolution image of the entire section (see supplementary Fig. 3). Using calibrated Image-Pro Plus software (Media Cybernetics Inc., MD, USA) we then measured the total length of each diaphragm along the basement membrane in order to adjust for any differences in size between diaphragms. Using the same software we then measured around each area of granuloma which were obvious. Areas of adherent tissue such as Liver, connective tissue or lymphatic tissue were not included in the measurement of granuloma tissue. Using the calibrated software we could then express the area of granuloma on each diaphragm (in mm^2) per unit length of diaphragm (in mm) to yield granuloma area per unit

diaphragm length (mm^2/mm). The results gained from diaphragms from a minimum of 3 separate animals for each treatment were analysed using one-way analysis of variance (ANOVA) with a Tukey-HSD multiple comparison post test. The data was then shown graphically in Figure 1d (raw data and statistical analysis shown in supplementary table 1 and 2 respectively) as a mean ± sem and values of $P < 0.05$ were considered significant.

SEM

The excised diaphragm was stained with osmium tetroxide prior to critical point drying, mounted and gold sputter coated before examination by scanning electron microscopy (SEM) using an Hitachi S-2600N digital scanning electron microscope (Oxford Instruments).

Statistics

We expressed all data as the mean ± s.e.m. and these were analysed using one-way analysis of variance (ANOVA). Multiple comparisons were analysed using the Tukey-HSD method and in all cases, values of $P < 0.05$ were considered significant.

Reference List

1. Davis, JM. *et al.* The pathogenicity of long versus short fibre samples of amosite asbestos administered to rats by inhalation and intraperitoneal injection. *Br. J. Exp. Pathol.* **67**, 415-430 (1986).

2. Graham, A., Higinbotham, J., Allan, D., Donaldson, K. & Beswick, PH. Chemical differences between long and short amosite asbestos: differences in oxidation state and coordination sites of iron, detected by infrared spectroscopy. *Occup. Environ. Med.* **56**, 606-611 (1999).

3. Singh, C., Shaffer, M., Kinloch, I. & Windle, A. Production of aligned carbon nanotubes by the CVD injection method. *Physica B: Condensed Matter* **323**, 339-340 (2002).

4. WHO Determination of airborne fibre number concentrations: a recommended method by phase contrast optical microscopy. *World Health Organisation* (1997).

5. Li, Q., Kinloch, IA. & Windle, AH. Discrete dispersion of single-walled carbon nanotubes. *Chem. Commun. (Camb.).* **26**, 3283-3285 (2005).

6. Sinani, VA. *et al.* Aqueous dispersions of single-wall and multiwall carbon nanotubes with designed amphiphilic polycations. *J. Am. Chem. Soc.* **127**, 3463-3472 (2005).

Supplementary Figures

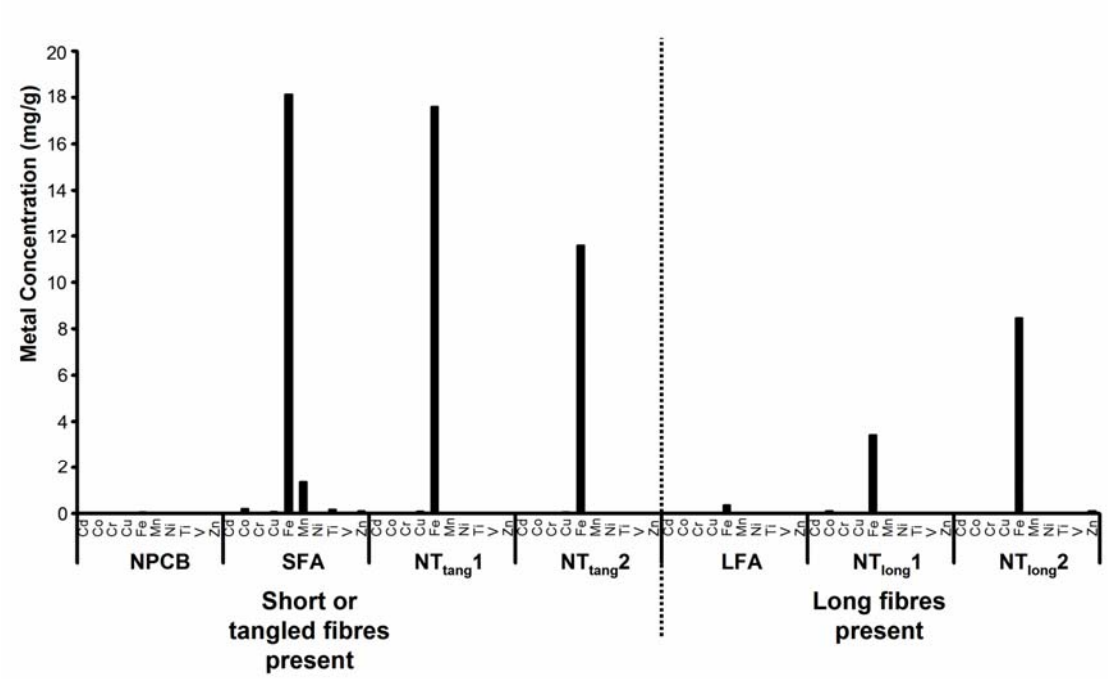

Supplementary Figure 1: Total metal contaminants of particle/ fibre panel. The total metal contamination of fibres/ particles utilised was established using inductively coupled plasma mass spectrometry (ICP-MS). The metal contaminants measured were cadmium (Cd), cobalt (Co), chromium (Cr), copper (Cu), Iron (Fe), Manganese (Mn), Nickel (Ni), Titanium (Ti), Vanadium (V) and zinc (Zn). The limit of detection for this assay was 0.0001mg/g.

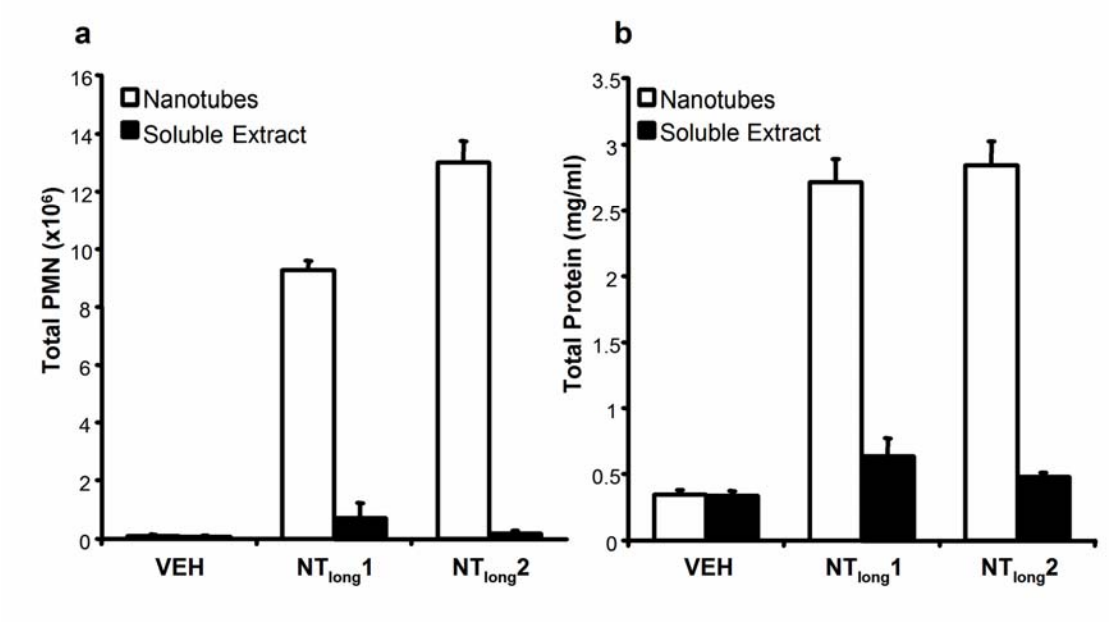

Supplementary Figure 2: Inflammatory cell recruitment to the peritoneal cavity after introduction of soluble fibre extract. A soluble fibre extract was prepared from samples NT_{long1} and NT_{long2} by overnight mixing in 0.5% BSA/ sterile saline vehicle. These extracts were then injected into the peritoneal cavity of female C57Bl/6 mice (0.5 ml; **VEH**, 0.5% BSA/ saline; 0.5 ml, **NT_{long1}** and **NT_{long2})**. Twenty four hours post exposure the mice were killed and the peritoneal cavity lavaged and the inflammatory response was evaluated using differential cell counts to establish total PMN population (**a,** mean±sem; n=3)) and total protein (**b**, mean±sem; n=3) indicating fluid exudation characteristic of inflammation. Comparison of the soluble extract to the vehicle control showed no significant increase in the total PMN population or protein levels in the peritoneal cavity (*P* 0.3652 and *P* 0.1160 respectively) after 24 hours.

a Vehicle Control (VEH)

VEH 1 of 4

– No granulomas

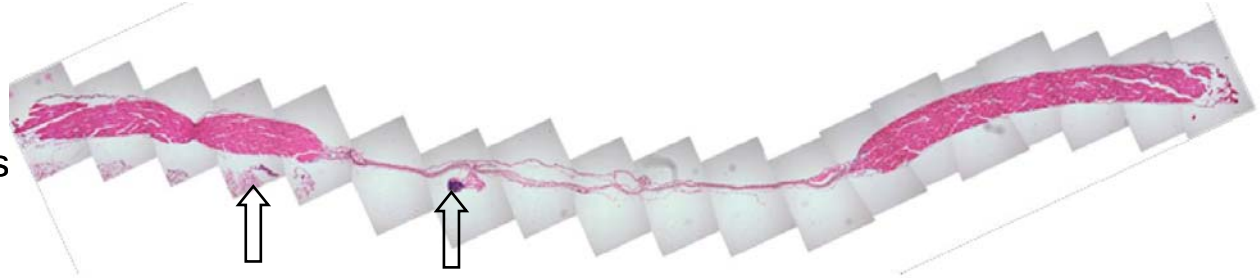

VEH 2 of 4

– No granulomas

VEH 3 of 4

– No granulomas

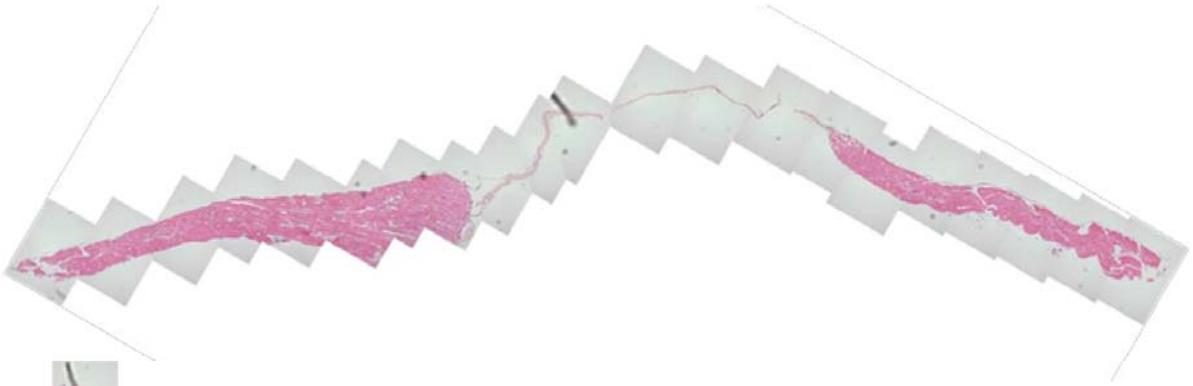

VEH 4 of 4

– No granulomas

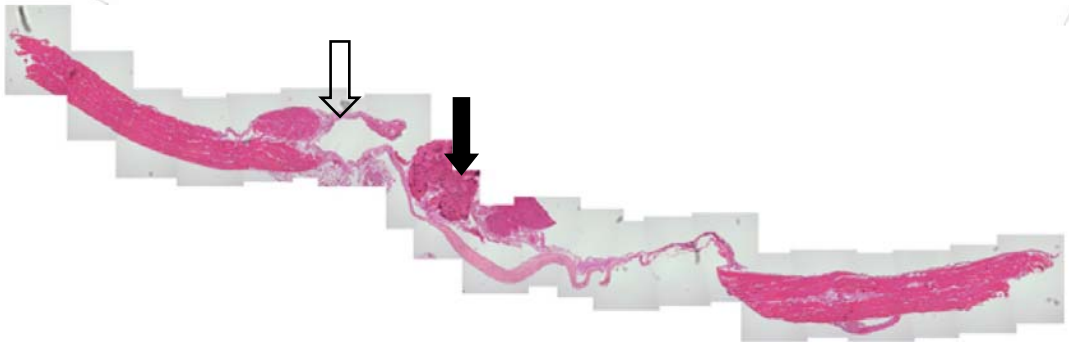

b Nano-Particulate Carbon Black (NPCB)

NPCB 1 of 3

– No granulomas

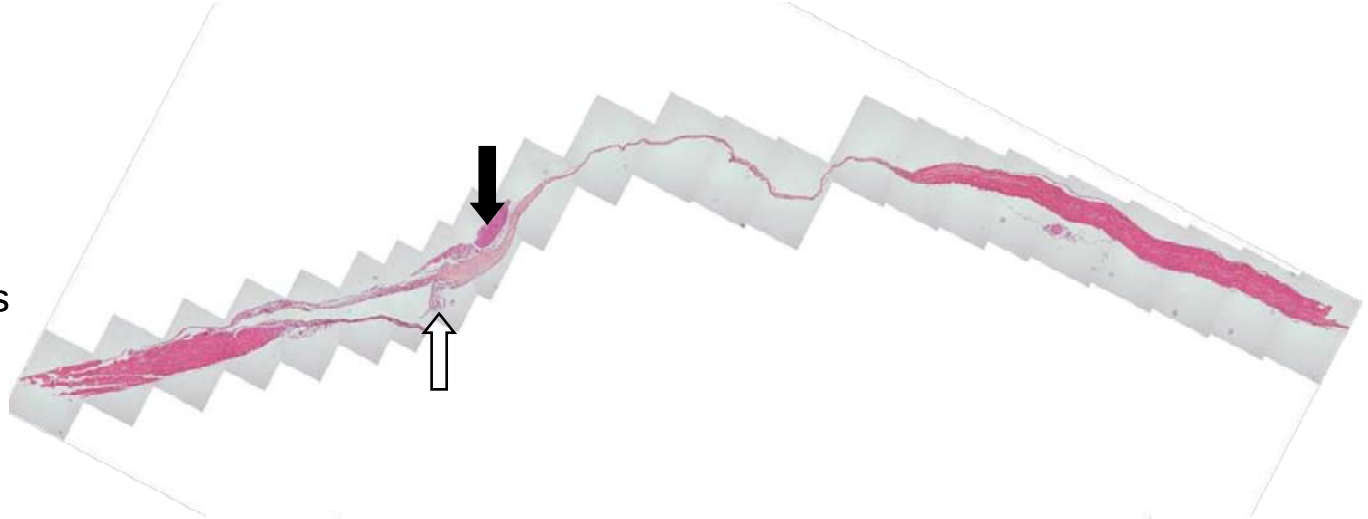

NPCB 2 of 3

– No granulomas

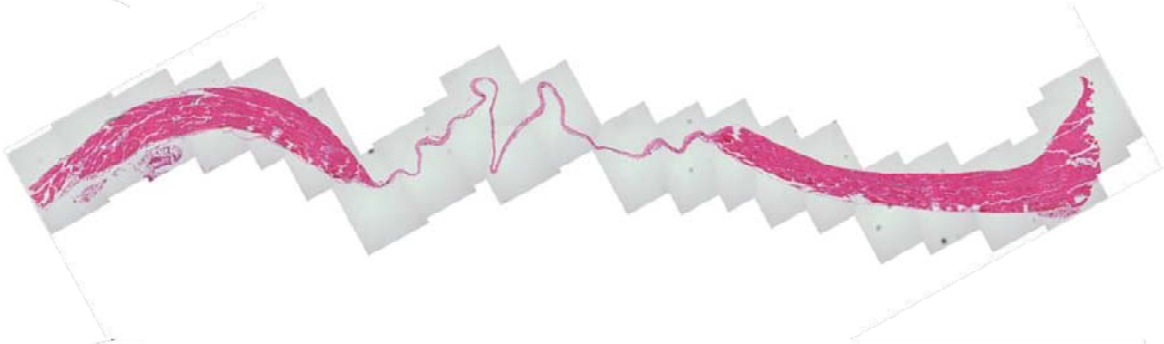

NPCB 3 of 3

– No granulomas

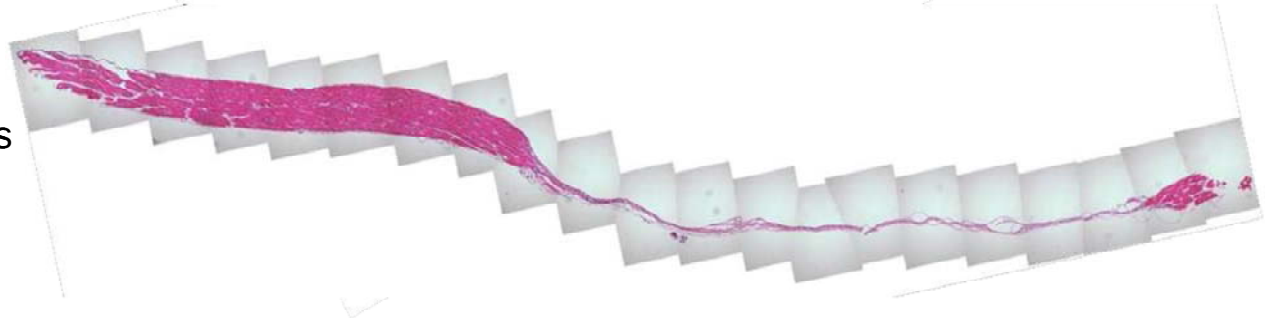

c Short Fibre Amosite (SFA)

SFA 1 of 3

– No granulomas

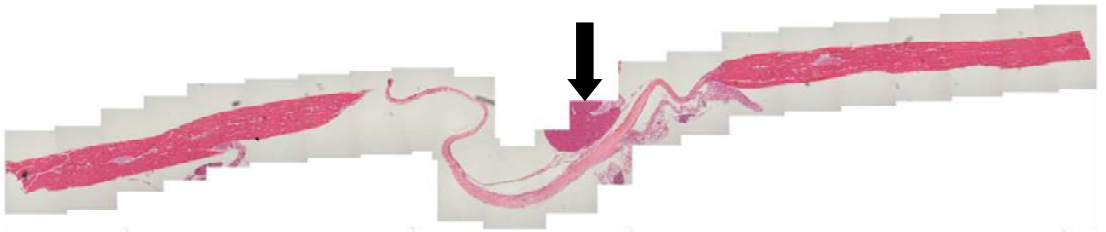

SFA 3 of 3

– No granulomas

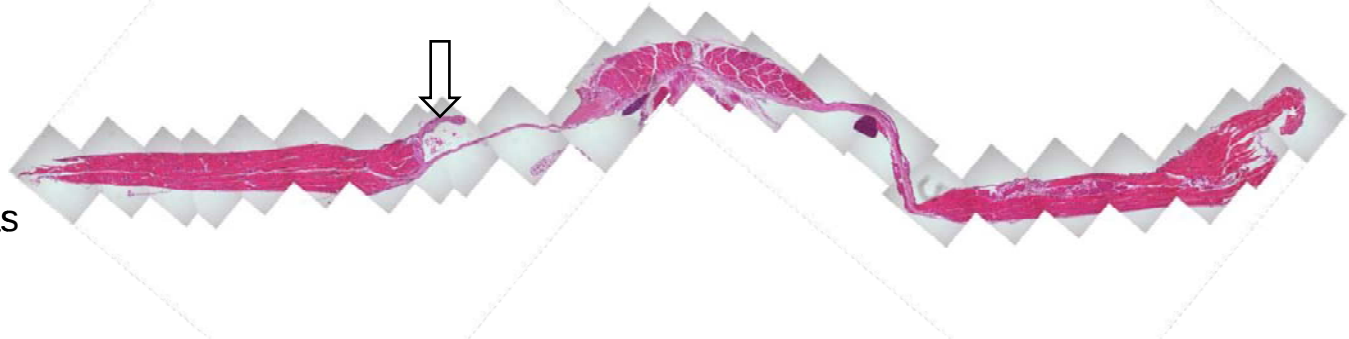

SFA 3 of 3

– No granulomas

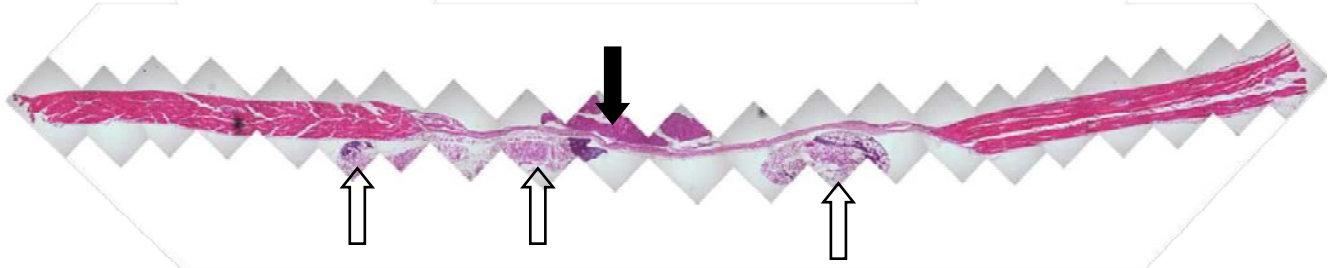

d NT_{tang1}

NT_{tang1} 1 of 3

– No granulomas

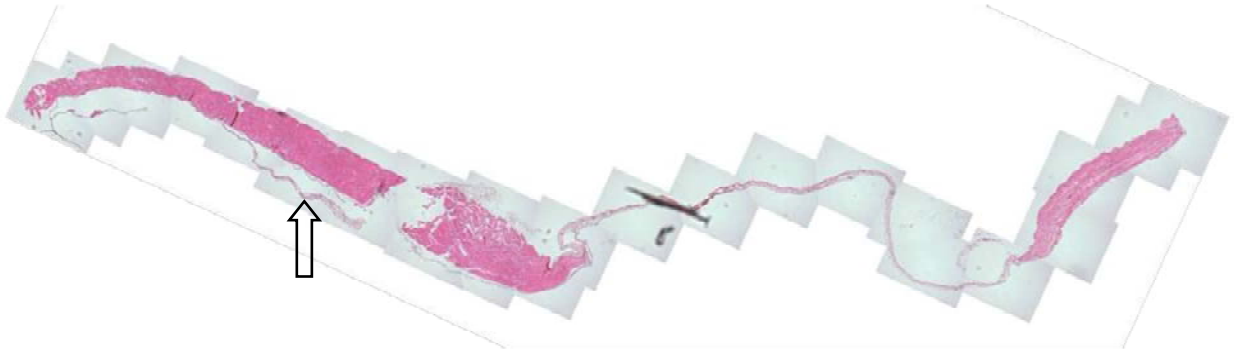

NT_{tang1} 2 of 3

– No granulomas

NT_{tang1} 3 of 3

– No granulomas

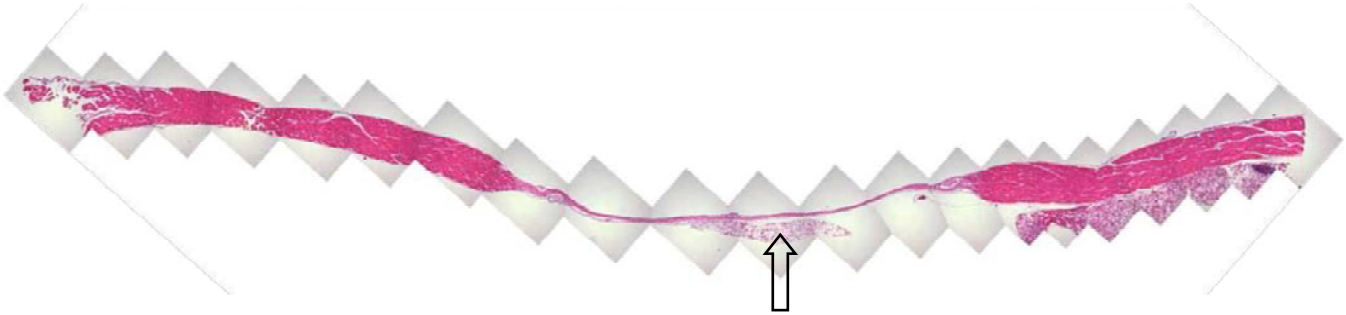

e NT_{tang2}

NT_{tang2} 1 of 3

– No granulomas

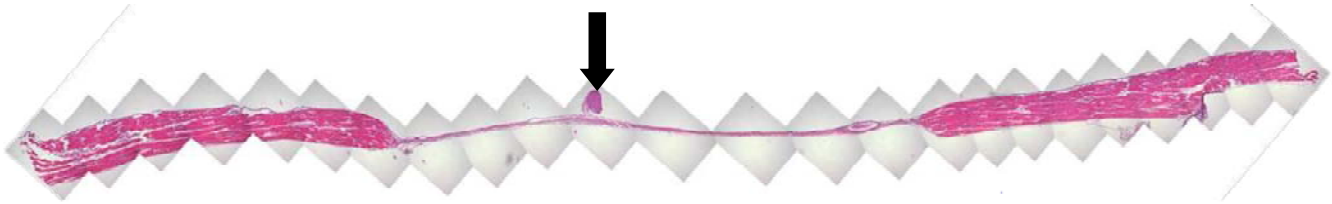

NT_{tang2} 2 of 3

– Discrete granulomas

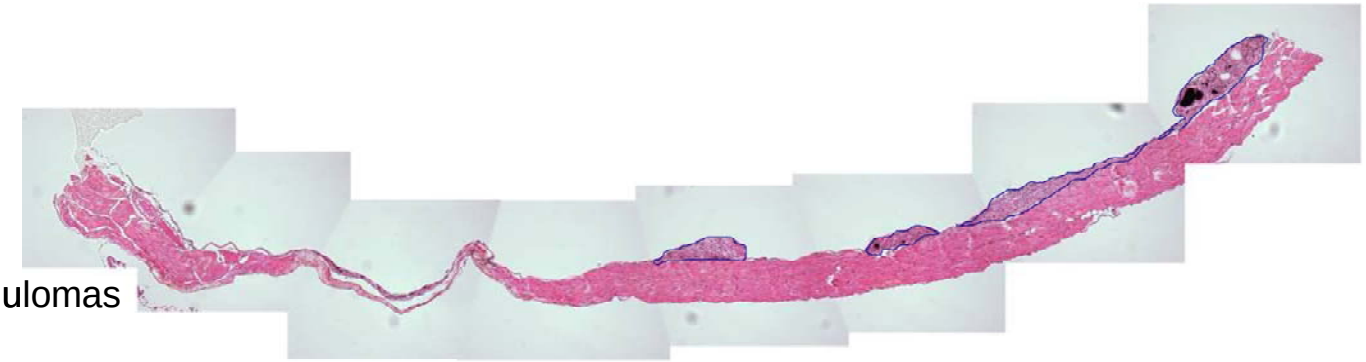

NT_{tang2} 3 of 3

– No granulomas

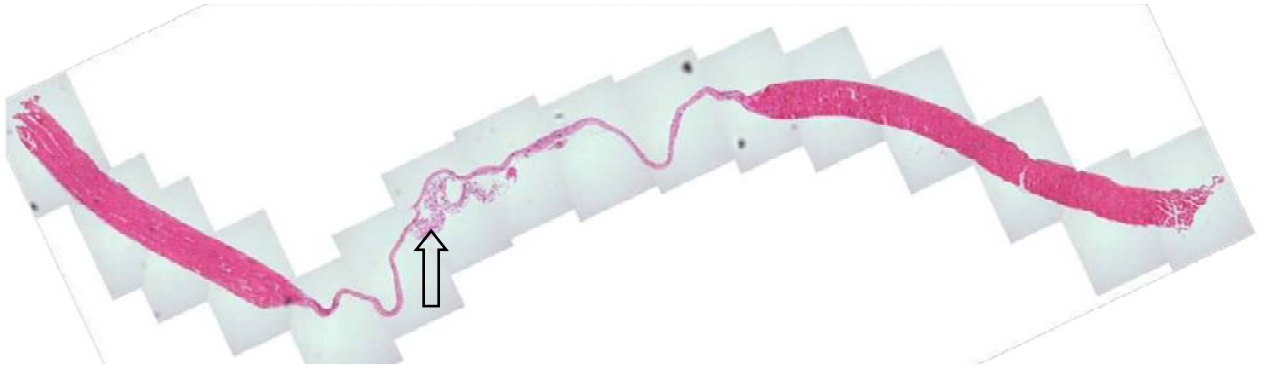

f Long Fibre Amosite (LFA)

LFA 1 of 3

– Extensive granulomas

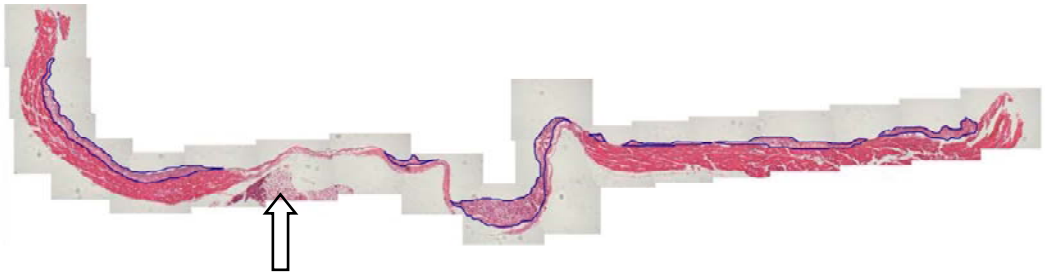

LFA 2 of 3

– Extensive granulomas

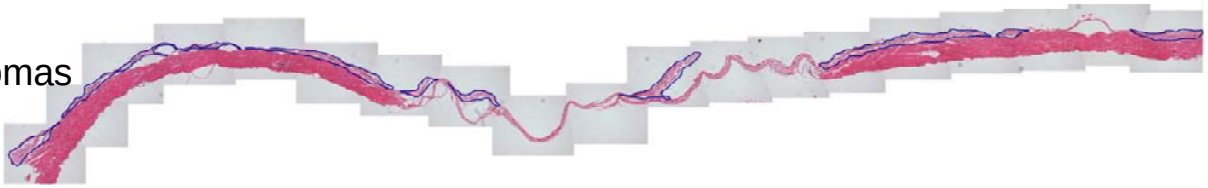

LFA 3 of 3

– Extensive granulomas

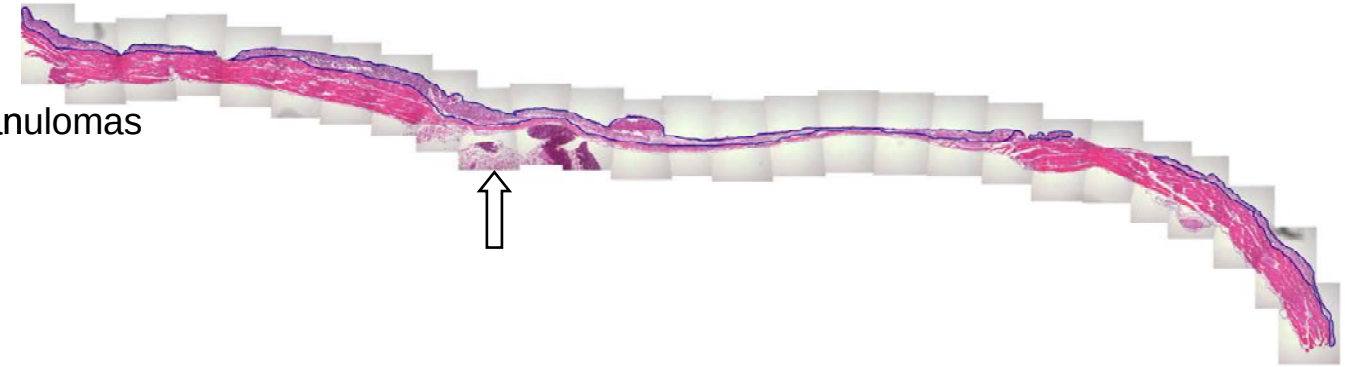

g NT_{long1}

NT_{long1} 1 of 4

– Extensive granulomas

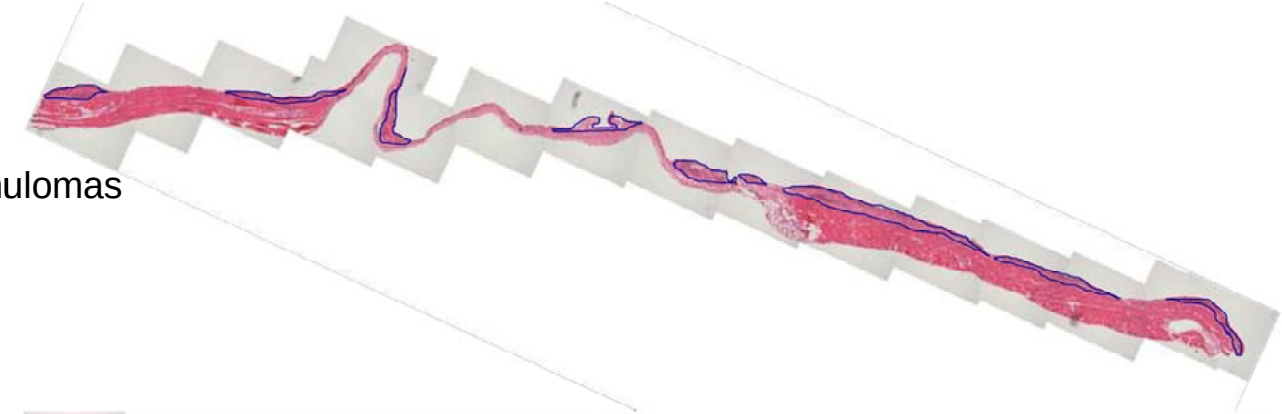

NT_{long1} 2 of 4

– Extensive granulomas

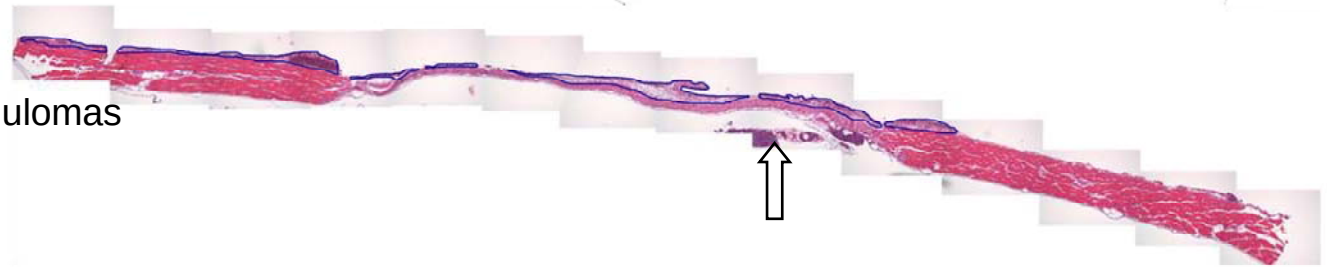

NT_{long1} 3 of 4

– Extensive granulomas

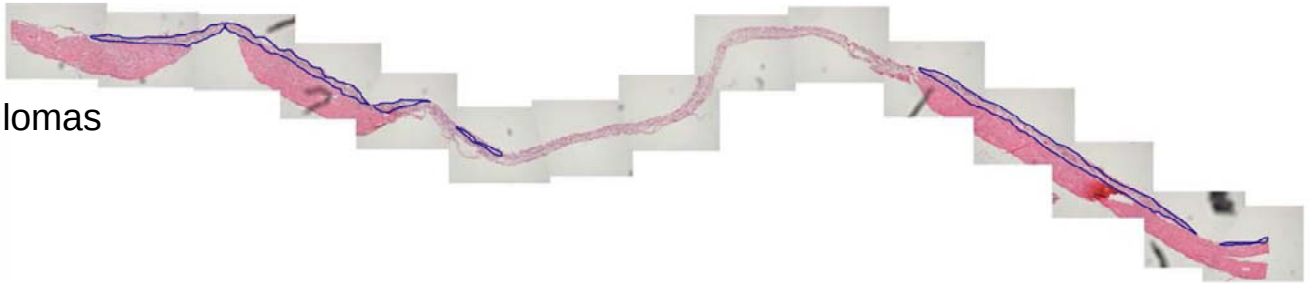

NT_{long1} 4 of 4

– Extensive granulomas

h NT_{long2}

NT_{long2} 1 of 3

– Extensive granulomas

NT_{long2} 2 of 3

– Extensive granulomas

NT_{long2} 3 of 3

– Extensive granulomas

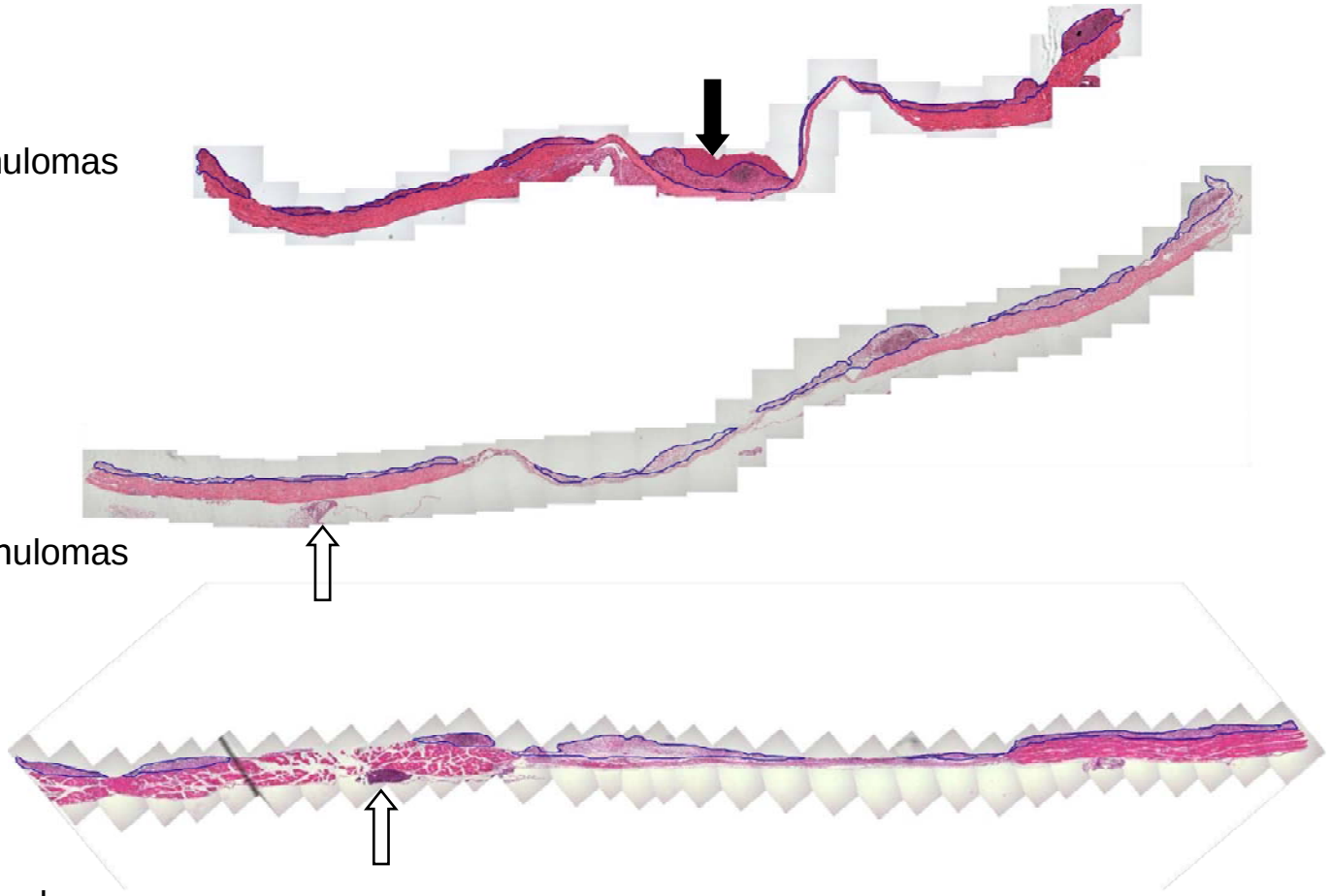

Supplementary Figure 3: Histology sections of mouse diaphragms.

Female C57BL/6 mice were treated with Vehicle control (**a**, 0.5% BSA/ Sterile saline; VEH 0.5ml; N = 4), NPCB (**b**, 50 µg; N = 3), SFA (**c**, 50 µg; N = 3), NT_{tang1} (**d**, 50 µg; N = 3), NT_{tang2} (**e**, 50 µg; N = 3), LFA (**f**, 50 µg; N = 3), NT_{long1} (**g**, 50 µg; N = 4) or NT_{long2} (**h**, 50 µg; N = 3) for 7 days with the peritoneal aspect shown upwards. Serial images were taken along the length of each diaphragm at x100 magnification and the images re-aligned using Photoshop elements 4.0 (Adobe systems Inc.). The areas of granuloma tissue (outlined in blue for clarity), demonstrated here in treatments e-h, were measured across each diaphragm section. This was conducted at high resolution using calibrated Image-Pro Plus software (Media Cybernetics Inc., MD, USA) to identify and measure any granuloma tissue via presence of inflammatory cells. Granuloma tissue was expressed as area (mm^2) per mm length of diaphragm and any areas of normal adherent tissue such as Liver (solid arrow) or connective tissue (hollow arrow) were not included in the measurement of granuloma. Extensive areas of Granuloma tissue were consistently induced by exposure to LFA (f), NT_{long1} (g) and NT_{long2} (h). A small granuloma response was observed in one out of three of the NT_{tang2}-treated mice (e, diaphragm 2 of 3) and subsequent analysis showed this to be a non-significant response (see main text for a full discussion and supplementary table 1 and 2 for raw data and statistical analysis respectively).

Supplementary Table 1: Raw morphometry data of the isolated diaphragms. Diaphragm lesion areas and overall diaphragm length was established using Image-Pro Plus software (Media Cybernetics Inc., MD, USA) for each diaphragm to enable the calculation of granuloma area per unit length of the diaphragm (**mm^2/mm)**.

Treatment	Granuloma Area (mm^2)	Diaphragm Length (mm)	Granuloma Area/ Unit Length (mm^2/mm)
VEH - 1	0.00	11.11	0.00
VEH - 2	0.00	11.66	0.00
VEH - 3	0.00	10.72	0.00
VEH - 4	0.00	9.24	0.00
NPCB - 1	0.00	11.72	0.00
NPCB - 2	0.00	12.25	0.00
NPCB - 3	0.00	10.43	0.00
SFA - 1	0.00	11.09	0.00
SFA - 2	0.00	14.08	0.00
SFA - 3	0.00	11.50	0.00
$NT_{tang}1$ - 1	0.00	12.08	0.00
$NT_{tang}1$ - 2	0.00	11.93	0.00
$NT_{tang}1$ - 3	0.00	11.01	0.00
$NT_{tang}2$ - 1	0.42	4.70	0.09
$NT_{tang}2$ - 2	0.00	7.88	0.00
$NT_{tang}2$ - 3	0.00	9.53	0.00
LFA - 1	1.98	11.11	0.18
LFA - 2	1.45	11.86	0.12
LFA - 3	3.32	13.15	0.25
$NT_{long}1$ - 1	1.80	10.27	0.17
$NT_{long}1$ - 2	1.67	10.10	0.16
$NT_{long}1$ - 3	1.11	9.13	0.12
$NT_{long}1$ - 4	0.90	9.39	0.10
$NT_{long}2$ - 1	3.59	11.38	0.32
$NT_{long}2$ - 2	3.14	13.55	0.23
$NT_{long}2$ - 3	4.05	13.45	0.30

Supplementary Table 2: One-way Analysis of Variance (ANOVA) performed on the raw morphometry data of the diaphragms in supplementary table 1. Statistical analysis was performed using InStat statistical software (GraphPad Software Inc.). A P value of < 0.0001 is considered extremely significant and variation among column means is significantly greater than expected by chance. A P value of >0.05 is considered non-significant. Tukey-Kramer Multiple Comparisons Test comparisons with the vehicle control (VEH) are shown: **Non-significant NT_{tang2} result boldened**

Comparison	Mean Difference	Q Value	P Value
VEH vs NPCB	0.000	0.000	ns P>0.05
VEH vs SFA	0.000	0.000	ns P>0.05
VEH vs NTtang1	0.000	0.000	ns P>0.05
VEH vs NTtang2	**-0.03000**	**1.603**	**ns P>0.05**
VEH vs LFA	-0.1833	9.798	*** P<0.001
VEH vs NTlong1	-0.1375	7.937	*** P<0.001
VEH vs NTlong2	-0.2833	15.142	*** P<0.001

ns = not significant